Study on Water Characteristic Curve of Unsaturated Red Clay

Song Chen
Key Laboratory of Urban Security and Disaster Engineering of Ministry of Education, Beijing University of Technology, Beijing, China

Abstract: Under the background of climate warming on the plateau regions, the freeze-thaw cycle has had a significant impact on issues such as slope stability. In this paper, three test methods were adopted to conduct soil-water characteristic curve tests on red clay in the southwest plateau region under various dry densities under freeze-thaw cycles. The fitting model of song was used to fit the test data to obtain the influence laws of freeze-thaw cycles and different dry densities on the suction force of soil samples, so as to provide a reference for engineering design. The test results show that the soil-water characteristic curves of red clay with different dry densities present a bimodal feature. Different dry densities and freeze-thaw cycles have a significant impact on the soil-water characteristic curves of red clay, and the influence is mainly concentrated in the low suction stage. The curves within the high suction force range almost coincide. The fitting degrees of the adopted fitting models were all >0.98, and the fitting was good.

Keywords: Red Clay; Freeze-Thaw Cycle; Direct Measurement Method; Shrinkage Characteristics; Fitting Mode

1. Introduction

The extreme and complex climate in the Nangqian area of the plateau region, with significant annual temperature differences, can cause freeze-thaw effects on soil, while notable temperature changes increase soil instability[1]. The uneven precipitation in plateau areas leads to variations in soil moisture content. In most engineering practices, surface soils are closely associated and generally exist in a non-saturated state, meaning that the pores between soil particles contain both liquid and gas. For example, some shallow landslides have soils that are in a non-saturated condition.

The water-soil characteristic curve is a crucial concept in unsaturated soil mechanics, describing the constitutive relationship between water content and matric suction in soil. Water content can be expressed as gravimetric water content, volumetric water content, or saturation. Through the water-soil characteristic curve, one can study the strength properties, deformation properties, and permeability characteristics of unsaturated soils [4].

For a saturated sample under a specific stress state, the internal pores of the sample consist of external pores and internal pores that are aggregated [5]. According to the characteristics of the soil-water characteristic curve, there are generally two segments with decreasing slopes and a relatively short horizontal transition zone in the middle section. The soil-water characteristic curve is classified into single-peak and double-peak soil-water characteristic curves based on the type of pore structure.

For soil samples with double pores, the full suction range soil-water characteristic curves of compacted expansive clay studied by Romero et al. [6] and Qian et al. [7] both exhibit clear bimodal features; Sun et al. [8] conducted full-range water-holding characteristic tests on red clay from Guilin, China, and the curves of compacted soil samples show significant bimodal characteristics. There is little reporting on the impact of large-scale freeze-thaw cycles on the water-holding characteristic curves of red clay.

The dual-peak characteristics of soil-water properties under freeze-thaw cycles and full suction range have attracted the attention of scholars. Ding et al. [9] established soil-water characteristic curves to analyze the effects of freeze-thaw cycles (FT) on the elastic modulus (MR), unconfined compressibility, and other mechanical properties of low-plasticity and high-plasticity loess subgrade soils; Zhao Guitao et al. [10]Ding et al. [11] conducted studies on the effects of drying and wetting processes, freeze-thaw cycles, and cement content on the microstructure, volume strain, and soil-water characteristic curves of cement-stabilized expansive soils; Fredlund et al. [12] provided a detailed summary of various testing methods for soil-water characteristic curves, along with their advantages and disadvantages. Testing methods are mainly divided into direct and indirect methods. Direct methods include the tensiometer method and the soil-water pressure plate method, while indirect methods include the filter paper method, steam balance method, and hygrometer method.

The Nangqian County in the plateau region has extensive red clay slopes. Therefore, it is urgently necessary to obtain the water and soil characteristic curves of red clay in the plateau region. To this end, this paper takes the red clay from Nangqian in the plateau region as the research object, conducting freeze-thaw cycle tests and subsequent soil-water characteristic curve tests after the freeze-thaw cycles, to reveal the influence patterns of freeze-thaw cycles on the water and soil characteristic curves of red clay.

2. Regional Overview

The study area is located in Nangqian County, Yushu Prefecture, Qinghai Province, in the eastern part of the plateau region, as shown in the figure, situated at approximately east longitude95 degrees and north latitude32 degrees. Nangqian County has an altitude of 3500-4500 m, with a climate characterized as typical continental monsoon. As illustrated in Figure 1, the study area, Nangqian County, is located in the southeastern part of the plateau region and falls within a typical seasonal permafrost zone.

3. Basic Physical Indicators

The test materials were taken from the landslide area of Nangqian County in the plateau region. After removing the surface vegetation soil, the soil was taken with a depth of about 0.2m. The basic physical properties of red clay were obtained based on the indoor test, and the test results are listed in Table 1.

According to the basic physical parameters of red clay measured on site, the initial water content is set at 24%, and two target dry densities are $1.5\ \mathrm{g/cm^3}1.6\ \mathrm{g/cm^3}$.

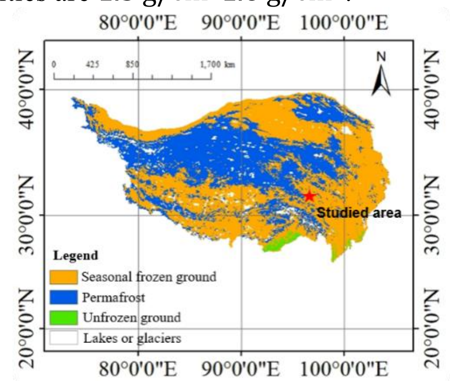

Figure 1. Distribution of Permafrost in the Plateau Area

Table 1. Basic Physical Properties of Red Clay

Natural water content w/(%)	Specific gravity of soil G_s partical	Natural density /()ρg·cm^{-3}	dry density /()ρ_dg·cm^{-3}	liquid limit I_L/(%)	plastic limit /(%w_P)
24.32	2.78	2.03	1.63	45.5	23.9

4. Test Process and Key Points of Operation

4.1 Soil Sample Treatment and Sample Preparation

During the experiment, soil samples taken from the site were pre-treated. First, the soil samples were air-dried and crushed to reshape them. Soil samples passing through a 2mm round hole sieve were used for sample preparation. When preparing the samples, first place the soil in an oven to dry for more than 24 hours to ensure all moisture has evaporated. Remove the soil from the oven and evenly spray it with a spray bottle until it is moistened. After moistening the soil to 24% moisture content, place it in a plastic sealed bag, ensuring there are no large clumps of soil. Let the moistened soil sit in a sealed environment for 24 hours. Before preparing the test samples, determine the moisture content using the drying method. Once the moisture content is accurate, proceed with the preparation. Use the static compaction method to compact wet red clay into ring knife samples, with dimensions of 20mm diameter and height 61.8mm.

At the same time, after all samples are prepared, the samples are prepared into saturated samples by vacuum method and then the next step of test can be carried out.

All samples require a freeze-thaw cycle test. According to the relevant test data, the freezing temperature in the constant temperature test chamber is set at-17℃ for 12 hours; the thawing temperature is set at 20℃ for 12 hours. The above process is considered one complete freeze-thaw cycle. The number of freeze-thaw cycles is set as 0, 1, 3, 5, and 7 [13].

4.2 Test Method of Soil and Water Characteristic Curve

In this experiment, three methods, namely axial translation technique, filter paper method and steam balance method, were used to obtain the complete soil-water characteristic curve of red clay. The three methods measured the low suction section from 0 to 500kPa, the medium suction section from 500 to 3000kPa and the high suction section 3.29~367.54MPa.

In the axial translation technique, the pressure paths applied to the sample inside the instrument are 0, 20 kPa, 40 kPa, 80 kPa, 160 kPa, 320 kPa, and 450 kPa. In this technique, only one sample is required to obtain the data on the relationship between moisture content and suction under these pressure paths; in the filter paper method, a contact test is used, where the three dry densities are saturated and then air-dried to corresponding moisture contents of 17%,14%,11%,8%, and 6%. The calibration curve obtained from the Whatman No.42 filter paper moisture content and Wang Fei's [14] test methods can be used to determine the matrix suction of the sample at different moisture contents.

The reference calibration equation is:

$$\log\psi = -0.0370\omega + 3.9825, \omega < 59.5\%$$
$$\log\psi = -0.0112\omega + 2.4423, \omega \geq 59.5\% \quad (1)$$

The former $\psi\omega$ is the substrate suction (kPa); the latter is the water content of the balanced filter paper (%)

In the sealed moisturizing tank, eight different saturated salt solutions were used to achieve eight constant humidity levels in the air, thereby obtaining the substrate suction [15] of red clay at different moisture contents. The saturated salt solutions and controlled suction values are shown in Table 2. The moisturizing tank can control the suction at 21.82,38.00,48.42,71.12,113.50,149.51,286.70, and 367.54MPa. After the samples stabilize, their moisture content is measured to obtain the stable moisture content. Therefore, eight samples need to be prepared for each soil-water characteristic curve.

5. Test Results

5.1 Soil Water Characteristic Curve

The water content obtained from the test is converted into saturation using a transformation $S_r = wG_s/e\, S_r - sS_r$formula, and a graph of the relationship between saturation and suction is plotted. As shown, this is the measured soil-water characteristic curve on the ()-saturation plane. As illustrated in Figure 2, as suction increases, there are three stages of change: with increasing suction, saturation first experiences a slow decline, then a sharp decrease, and finally stabilizes gradually. The soil-water characteristic curves at three different dry densities all show a second peak around 2800 kPa, indicating that the red clay soil-water characteristic curve exhibits a bimodal feature. This is prominently displayed in subsequent fitting images.

Table 2. Relative Humidity and Suction above Different Closed Saturated Salt Solutions at 25°C

Name of the salt solution	relative humidity /%	Total suction /KPa
Lithium chloride solution	12.0	286700
Magnesium chloride solution	33.1	149510
Potassium carbonate solution	43.2	113500
Sodium bromide solution	59.1	71120
liquor kalii iodidi	69.9	48420
sodium chloride solution	75.5	38000
Klorvess Liquid	85.1	21820
Potassium sulfate solution	97.6	3290

The impact of freeze-thaw cycles $S_r - sS_r$与$s$on the relationship is evident within the low suction range. When s <2 MPa, the relationship decreases as the number of freeze-thaw cycles increases. This may be related to the damage caused by freeze-thaw cycles to the soil's pore structure. When s> 2 MPa, soil samples show almost overlapping behavior under different freeze-thaw cycles.

The main reason is that in the high suction stage, the water in the soil pores is mainly adsorbed water [3]. The existence of adsorbed water is mainly related to mineral composition, and the adsorption moisture content is less affected by the change of soil sample structure. The maximum adsorption moisture content does not depend on dry density [2].

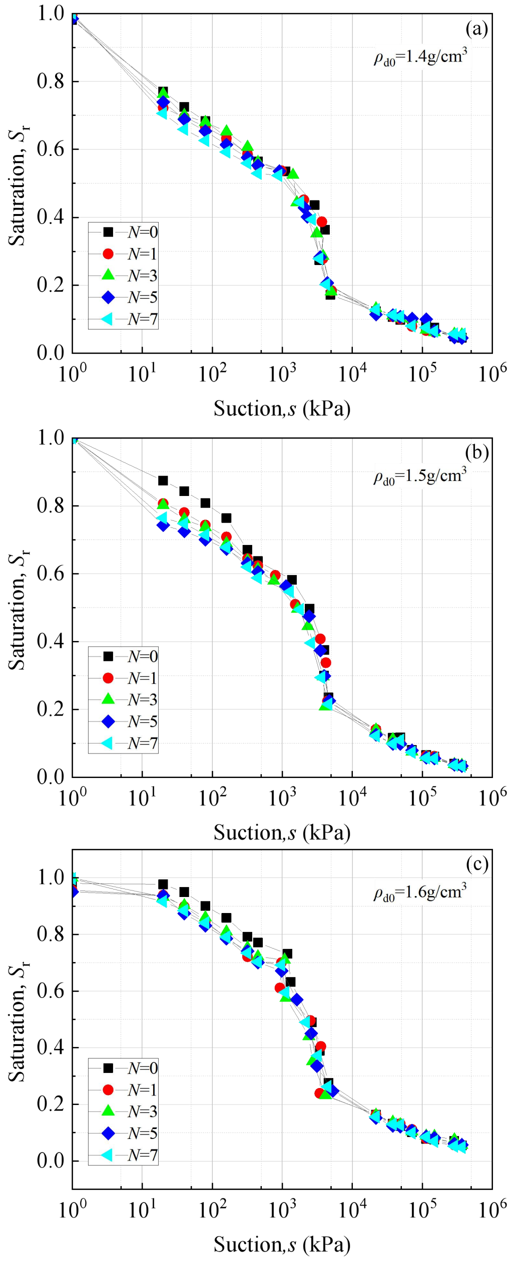

Figure 2. Soil-water Characteristic Curves of Three Dry Densities under the Action of Freeze-thaw Cycles

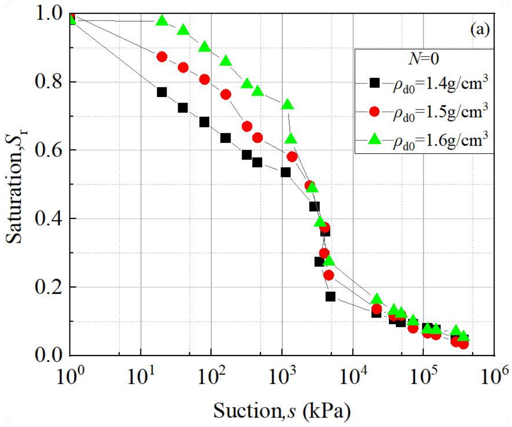

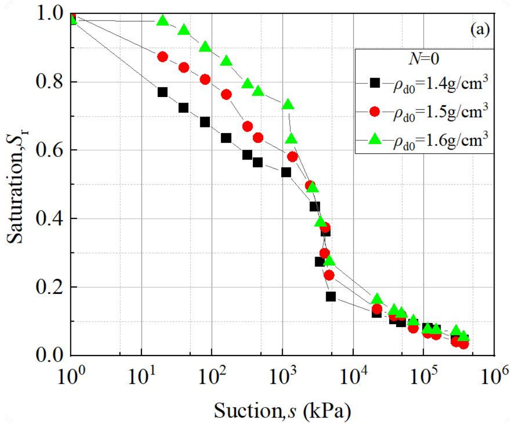

Figure 3. The Soil-water Characteristic Curves of Three Dry Densities under the Same Freeze-thaw Cycle

Here, further analysis and discussion of the initial dry density relationship of red clay within the full suction range are presented $S_r - sS_r - sS_r - sS_r - sS_r - sS_r - s$. Figures 3(a) and 3(b) show the relationships between three different initial dry densities of compacted red clay samples under freeze-thaw cycles N=0 and N=7, respectively. In the low suction range, the initial dry density also has a significant impact on the relationship. For samples with N=0, the influence of initial dry density is mainly reflected in the suction range of 4000 kPa. For samples with N=7, the influence of initial dry density is evident in the s range of 2600 kPa. Therefore, the effects of freeze-thaw cycles and initial dry density on the relationship between experimental compaction and red clay are primarily observed in the low suction range.

5.2 Fitting Equation

In this chapter, the experimental data will be fitted by the bimodal soil-water characteristic curve fitting equation proposed by Song, Zhang et al., which considers the initial porosity ratio and capillary and adsorption effects.

In this model, it is believed that the pore water consists of two parts, namely adsorption water and capillary water

$$S_r = S_{ra} + S_{rc} \tag{2}$$

In the formula, Sr is saturation, Sra is water saturation and Src is capillary water saturation.

In summary, to simplify the fitting process and better analyze the soil-water characteristic curves α under freeze-thaw cycles, the simplified model will be used as the model parameters, without considering the influence of the initial porosity. Therefore, Equation (3) is converted into the new adsorption water-holding curve equation (5), and Equation (4) is converted into the new capillary water-holding curve model (6):

In the formula, S_{ra}^{max}Sra is the maximum value, in which the change of porosity during soil shrinkage is not considered, so (3) is changed to the form in (5).

$$S_{ra} = S_{ra0}^{max}\left(\frac{e_0}{e}\right)\left\{1-\left[\exp\left(\frac{s-s_{max}}{s}\right)\right]^m\right\} \quad (3)$$

$$S_{rc} = \frac{1}{2}\left[1-erf\left(\sqrt{2}\frac{s-s_c}{s_c}\right)\right]\left[1-S_{ra}\right]\left\{1+\left[\alpha_0\left(\frac{e}{e_0}\right)^b s\right]^n\right\}^{1/n-1} \quad (4)$$

$$S_{ra} = S_{ra0}^{max}\left\{1-\left[\exp\left(\frac{s-s_{max}}{s}\right)\right]^m\right\} \quad (5)$$

$$S_{rc} = \frac{1}{2}\left[1-erf\left(\sqrt{2}\frac{s-s_c}{s_c}\right)\right]\left[1-S_{ra}\right]\left\{1+\left[\alpha s\right]^n\right\}^{1/n-1} \quad (6)$$

There are seven parameters in the model, which can be classified according to the equation. There are three parameters $S_{ra0}^{max} s_{max}$ $s_c \alpha s_{max}$ in the adsorption equation:, and m, and four parameters in the capillary action equation:,, b and n. It can be regarded as the maximum suction range of 106 kPa, so there are six parameters that need to be determined by fitting the original data.

Because the parameter $\alpha\alpha$ is a fitted parameter associated with the air intake value AEV, its reciprocal 1/ directly represents the air intake value (AEV). The parameter is related to the shape of the soil-water characteristic curve for the capillary water action part, reflecting changes in the position of the air intake value (AEV) during the low suction phase. This further indicates how freeze-thaw cycles affect the air intake value of soil types or pore structures. Under freeze-thaw cycles, a decrease in air intake value corresponds to a reduction in the parameter, suggesting that freeze-thaw action may lead to pore expansion or micro-crack formation, making the soil more prone to drainage under low suction and reducing its water retention capacity.

For soil samples with the same dry density, the suction exceeds 2800kPa until reaching the high-suction stage. The suction generated by adsorbed water gradually becomes the primary influence. The presence of adsorbed water is related to [16], which is less affected by pore structure. This indicates that micro-pores produced by freeze-thaw cycles have a minimal impact on the existence of adsorbed water. The results are consistent with those from soil-water characteristic curve tests, and the curves tend to overlap with each other at different freeze-thaw cycle frequencies

Therefore, when performing the fitting, first fit and obtain the parameters of the soil-water characteristic curve for three dry densities under N=0 freeze-thaw cycles. For subsequent $\alpha S_{ra0}^{max} s_{max} s_c \mathrm{R}^2 R^2$ data fitting of freeze-thaw cycles, the parameters are not fixed; instead, the other fitting parameters and, are used their values at N=0 for data fitting. The fitted curves are shown in Figure 4, and the fitting parameters are listed in Table 3, with all fitting degrees exceeding 97%. The fitting degrees of the soil-water characteristic curves for the three dry density soil samples are all above 95%, indicating good fitting.

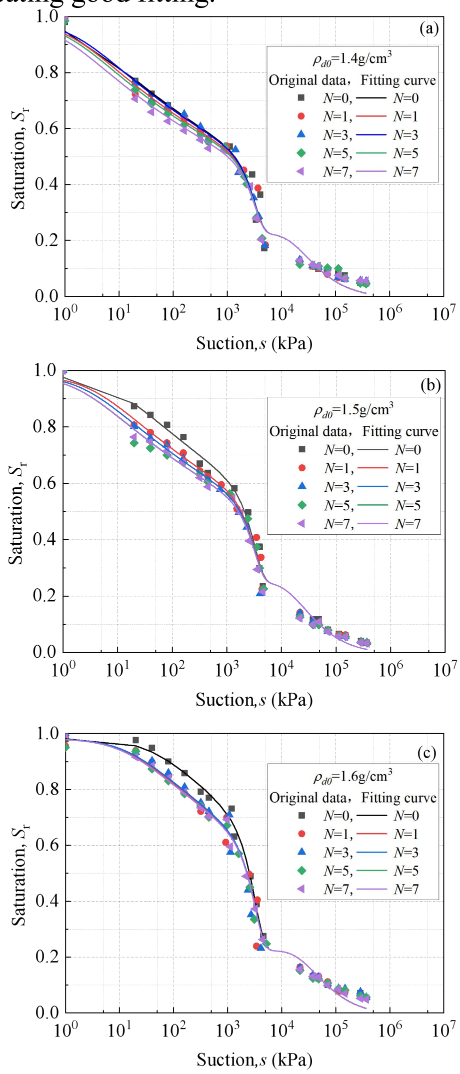

Figure 4. The Fitting Results of Soil-Water Characteristic Curves with Three Dry Densities

Table 3. The Fitting Parameters of Soil-Water Characteristic Curve

dry density $/(\rho_d g/cm^3)$	Fit parameters	Number of freeze-thaw cycles N	Proposed parameters α:(kPa-1)	R^2
1.4	$=0.22402S_{ra0}^{max}$	0	0.53761	0.98203
	$=100000s_{max}0kPa$	1	0.71692	0.9861
	m=0.03039	3	0.58402	0.99045
	$=2800s_c kPa$	5	0.84689	0.98955
	n=1.13137	7	1.17203	0.95593
1.5	$=0.24795S_{ra0}^{max}$	0	0.11357	0.99284
	$=100000s_{max}0kPa$	1	0.26669	0.9919
	m=0.027	3	0.34535	0.99275
	$=3000s_c kPa$	5	0.46423	0.99111
	n=1.13134	7	0.45721	0.99245
1.6	$=0.22255S_{ra0}^{max}$	0	0.02114	0.99567
	$=100000s_{max}0kPa$	1	0.06375	0.9867
	m=0.04406	3	0.06015	0.98618
	$=3000s_c kPa$	5	0.06984	0.99432
	n=1.1187	7	0.06984	0.9999

As shown in Figure 4, the values at three dry densities $\alpha\alpha g/cm^3 g/cm^3 \alpha$ all exhibit a pattern of increasing with the number of freeze-thaw cycles. This indicates that freeze-thaw action may lead to pore expansion or micro-crack formation, making the soil more prone to drainage under low suction and reducing its water retention capacity. Among them, the fitting parameters for 1.5 and 1.6 are closer when N=5 and N=7, which corresponds to the phenomenon in Figure 2 where the soil-water characteristic curves at low suction under freeze-thaw cycles almost coincide for the three dry densities. This suggests that the impact of freeze-thaw cycles on the soil samples stabilizes at N=5 and N=7.

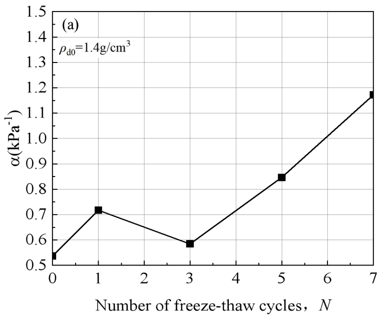

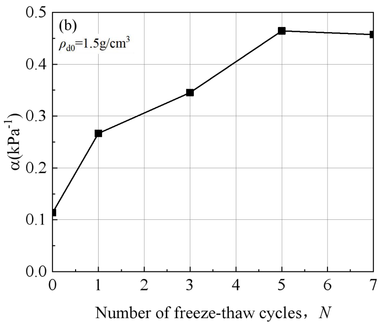

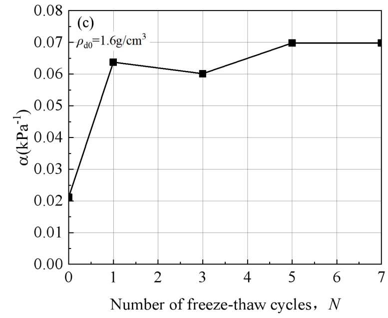

Figure 5. Value Variation under Freeze α-thaw Cycle

1.4 The initial porosity $g/cm^3 \alpha g/cm^3$ e is large and the value changes greatly, indicating that the freeze-thaw cycle has a great influence on the pore structure. The left shift of the low suction section curve is large, and the gas intake value is significantly reduced, and the water holding capacity decreases more violently. However, the initial porosity e of high dry density 1.6 is small, and the first freeze-thaw cycle has a significant effect, and then the influence gradually weakens.

6. Conclusion

The water characteristic curves of three types of dry density red clay after freeze-thaw cycles exhibit bimodal features. The water characteristic curve of compacted red clay shows a three-stage change: as suction increases, the water content sequentially experiences a slow decline, a sharp decrease, and then gradually stabilizes. Freeze-thaw cycles have a significant impact on capillary water, while adsorption water is less affected. When suction is below 2 MPa, the saturation decreases with increasing freeze-thaw cycles.

The influence of dry density and freeze-thaw cycle on the $S_r - sS_r - s$ soil water characteristic curve of red clay mainly focuses on the low suction stage. In the high suction range, the relationship between different dry densities and frozen-thaw cycle of compacted red clay samples is almost overlapping.

Using the fitting parameters of the soil-water characteristic curve for three dry densities αααwith N=0 freeze-thaw cycles, the soil-water characteristic curve was fitted under the remaining freeze-thaw cycles without fixing the parameters. The fitting degree R^2>0.98 for all soil-water characteristic curves, and the values at three dry densities showed a consistent pattern of increasing with the number of freeze-thaw cycles.

This paper innovatively studies the soil and water characteristic curve of red clay under the background of climate warming, which provides an important parameter basis for the stability of soil in highland slope engineering.

References

[1] DU Jun, LU Hongya, JIAN Jun. Variations of extreme air temperature events over Tibetfrom 1961 to 2010[J]. Acta Geographica Sinica, 2013, 68(09): 1269-1280.

[2] Sun, D.A., Gao, Y., Zhou, A.N., Sheng, D.C., 2016. Soil–water retention curves and microstructures of undisturbed and compacted Guilin lateritic clay. Bull. Eng. Geol. Environ. 75, 781–791.

[3] Baker R, Frydman S (2009) Unsaturated soil mechanics: critical review of physical foundations. Eng Geol 106(1-2):26–39.

[4] Sun De'an, Gao You, Liu Wenjie, et al. Soil and water properties of red clay and its pore distribution [J]. Journal of Geotechnical Engineering, 2015,37(02):351-356.

[5] CASINI F, VAUNAT J, ROMERO E, DESIDERI A. Consequences on water retention properties of double-porosity features in a compacted silt[J]. Acta Geotechnica, 2012, 7(2): 139-150.

[6] ROMERO E, GENS A, LLORET A. Water permeability, water retention and microstructure of unsaturated compacted Boom clay[J]. Engineering Geology, 1999, 54(1-2): 117-127.

[7] QIAN J, LIN Z, SHI Z. Experimental and modeling study of water-retention behavior of fine-grained soils with dual-porosity structures[J]. Acta Geotechnica, 2022, 17(8): 3245-3258.

[8] SUN D, YOU G, Annan Z, et al. Soil–water retention curves and microstructures of undisturbed and compacted Guilin lateritic clay[J]. Bulletin of Engineering Geology and the Environment, 2016, 75: 781-791.

[9] DING L, HAN Z, ZOU W, et al. Characterizing hydro-mechanical behaviours of compacted subgrade soils considering effects of freeze-thaw cycles[J]. Transportation Geotechnics, 2020, 24: 100392.

[10] Zhao Guitao, Han Zhong, Zou Weilie, et al. Effects of dry-wet and freeze-thaw cycles on soil-water and shrinkage characteristics of expansive soils [J]. Journal of Geotechnical Engineering, 2021,43(06):1139-1146.

[11] DING L, VANAPALLI S K, ZOU W, et al. Freeze-thaw and wetting-drying effects on the hydromechanical behavior of a stabilized expansive soil[J]. Construction and Building Materials, 2021, 275: 122162.

[12] Fredlund D G, Rahardjo H. Soil mechanics for unsaturated soils[M]. John Wiley and Sons, New York: New York, 1993.

[13] YU Y, ZHANG Z, DAI F, et al. A New Shear Strength Model with Structural Damage for Red Clay in the Qinghai-Tibetan Plateau[J]. Applied Sciences, 2024, 14(8): 3169.

[14] Wang Fei. Development of unsaturated soil column test device and study on capillary retardation type seepage prevention layer parameters [D]. Beijing: Beijing Jiaotong University, 2017.

[15] GREESPAN L. Humidity fixed points of binary saturated aqueous solutions[J]. Journal of Research of the National Bureau of Standards, 1977, 81(1): 89–96.

